J. Earth Syst. Sci. (2019)128 212
https://doi.org/10.1007/s12040-019-1245-z

Uranium enrichment at North Almora Thrust Zone, Kumaun Lesser Himalaya, Uttarakhand, India

Gaurav Joshi[1,*], K K Agarwal[1], Amar Agarwal[2] and J R Vidal-Solano[3]

[1] *CAS in Geology, University of Lucknow, Lucknow 226 007, India.*
[2] *Institute of Earth and Environmental Sciences, Geology, University of Freiburg, Freiburg, Germany.*
[3] *Departamento de Geología, Universidad de Sonora, Hermosillo, Mexico.*
**Corresponding author. e-mail: gaurav.j1988@gmail.com*

MS received 4 December 2018; revised 7 May 2019; accepted 13 June 2019

Intensely deformed and mylonitised rocks of the Almora Crystalline Zone (ACZ) have shown the potential of ^{238}U and ^{232}Th enrichment. ^{232}Th, ^{238}U and ^{40}K are investigated by gamma-ray spectrometry in the rock samples collected along the three selected traverses across the North Almora Thrust Zone (NATZ). Obtained average values of U and Th are much higher, 7.3 and 23.9 ppm, respectively, than the average upper crustal abundances (2.8 and 10.7 ppm). The Th/Ra(eU) varies between 2.1 and 23, indicating a higher concentration of Th. The enrichment is due to the remobilisation of the radioisotopes due to the intense mylonitisation and metamorphism from the granitic protolith. The zones of enrichment, although concentrated near NATZ, show a heterogeneous distribution.

Keywords. Kumaun Lesser Himalaya; Almora Crystalline Zone; North Almora Thrust Zone; Uranium enrichment; Spectrometry.

1. Introduction

Uranium deposits form in deep magmatic to subareal geological conditions, and range in age from the Archaean to recent times. However, understanding the various geological conditions under which U deposits form has remained challenging (Cuney 2009). This study presents an interesting case of ^{238}U, ^{232}Th and ^{40}K enrichment at a thrust zone in the Lesser Himalaya, India.

Numerous shear zones in the world have well-established U deposits, due to U-bearing fluids and/or volume loss, e.g., Singhbhum shear belt and the south Purulia shear zone in India and Mary Kathleen shear zone in Australia (e.g., Bhola *et al.* 1966; Oliver *et al.* 1999; Banerjee *et al.* 2011; Biswas and Sharma 2016).

Previous studies postulate U enrichment around the study area by reporting high radon concentration in springs, fractures, fault-lineament and shear zones of the north-central part of the Kumaun Lesser Himalaya (Choubey *et al.* 2000). The granitic rocks and their metamorphism products of the Saryu Formation, outcropping near the North Almora Thrust Zone (NATZ), also show high radon concentration (Choubey *et al.* 1999; Prasad *et al.* 2008). Furthermore, granites are known to be often enriched in U and Th (Florou and Kritidis 1992; Banerjee *et al.* 2011).

Supplementary material pertaining to this article is available on the *Journal of Earth System Science* website (http://www.ias.ac.in/Journals/Journal_of_Earth_System_Science).

The present study employs spectrometric analysis to identify the ^{238}U, ^{232}Th and ^{40}K concentrations at the NATZ along three selected traverses. The investigated rocks belong to the Almora Crystalline Zone (ACZ), which is one of the largest zones of deformed, metamorphosed and sheared granites and granitoids in the Lesser Himalaya (Bhattacharya and Agarwal 1985).

2. Geology of the area

The ACZ is a synform with axial plane trending almost WNW–ESE, dipping 60–65° due north and the fold axis gently plunging by 10–15° towards ESE (Joshi *et al.* 2017). Due to the ACZ's synformal structure, most of the foliations near the NATZ dip 24–60° to the south (Agarwal 1994). The ACZ is separated in the north from the Damtha–Tejam Group (part of LHS) by the south dipping NATZ, which is marked by well-defined zones of mylonites formed during the southward thrusting of the crystalline rocks (Valdiya 1980; Bhattacharya and Agarwal 1985; Agarwal *et al.* 2017). The study area exposes the northern part of the ACZ, along with NATZ and a variety of rock types such as schists, gneisses and mylonites, some of which are 1865 ± 50 Ma old (Rb/Sr whole rock ages by Trivedi *et al.* 1984).

3. Methodology

The spectrometric analysis was done on the samples studied in detail by Agarwal *et al.* (2016) and Joshi *et al.* (2017). The oriented samples were collected across the NATZ along three selected traverses, namely, Manan–Someshwar, Kapar Khan–Kaphaligair and Dhaul Chhina–Seraghat sections (figure 1).

^{40}K, ^{238}U and ^{232}Th decay series have radioisotopes that produce gamma rays of sufficient energy and intensity to be measured by gamma-ray spectrometry because of their relative abundance in the natural environment (Erdi-Krausz *et al.* 2003). The gamma spectrum for each sample is acquired for 4000 s and three iterations. For this, the rock samples are first crushed and radiometrically analysed to estimate their gross radioactivity content, i.e., equivalent uranium (eU_3O_8) concentration (hereafter designated by eU). If the concentration of the radioisotopes is <100 ppm, further investigations are done. Four hundred grams of the sample is crushed to −150 mesh size for estimating the content of individual radioisotopes, such as the equivalent radium concentration $Ra(eU_3O_8)$, henceforth designated as Ra(eU). It is estimated by counting 1.76 MeV gammas from ^{214}Bi of the Ra-group element belonging to U-series with an assumption that the U-series is in secular equilibrium. Ra(eU), thorium (ThO_2) and potassium (K%) concentrations are estimated using gamma-ray spectrometry in a multi-channel analyser (dMCA) with a $5 \times 4''$ NaI(Tl) detector coupled with a 2K MCA digital processing system (see Kukreti and Sharma 2012 for details) at physics laboratory, Atomic Minerals Directorates for Exploration and Research, Department of Atomic Energy, Northern Region, New Delhi, India. The windows are set up using ^{137}Cs and ^{60}Co standards for K, U and Th to calibrate the gamma-ray spectrometer and its channels. Bands of 1.36–1.56, 1.66–1.86 and 2.42–2.82 MeV were analysed to estimate the concentration of K, Ra(eU) and Th, respectively. This method achieves very high sensitivity leading to detection limits for eU < 10 ppm, $^{40}K < 1.0\%$, Ra(eU) < 2 ppm and Th < 2 ppm (Knoll 2000). All the concentrations, eU, Ra(eU) and Th, except ^{40}K are measured in ppm. The concentration of ^{40}K is expressed in ppm by converting the percentage into the ^{40}K content. This is done by using its natural abundance of 0.0118%, which implies that 1% ^{40}K is equivalent to 1.18 ppm of ^{40}K (Acharyulu *et al.* 2004).

4. Results

4.1 *Potassium, Uranium and Thorium concentration*

K, an alkali metal, has a tendency to concentrate in evolved crystalline rocks such as granites. During melting in the mantle and basalt differentiation, it remains incompatible, and, as a consequence, it is enriched in felsic igneous melts along with other incompatible elements such as Th and U (Guagliardi *et al.* 2013). Several rock-forming minerals like K-feldspars and micas have K as a major constituent.

^{40}K distribution in the study area is presented in figure 1(a). Metamorphosed and mylonitised rocks of the ACZ have much higher ^{40}K concentration as compared to the quartzite of the Rautgara Formation, in which the concentration is below the detection level. Among the ACZ rocks, the mylonites show lower ^{40}K concentration, between 1 and

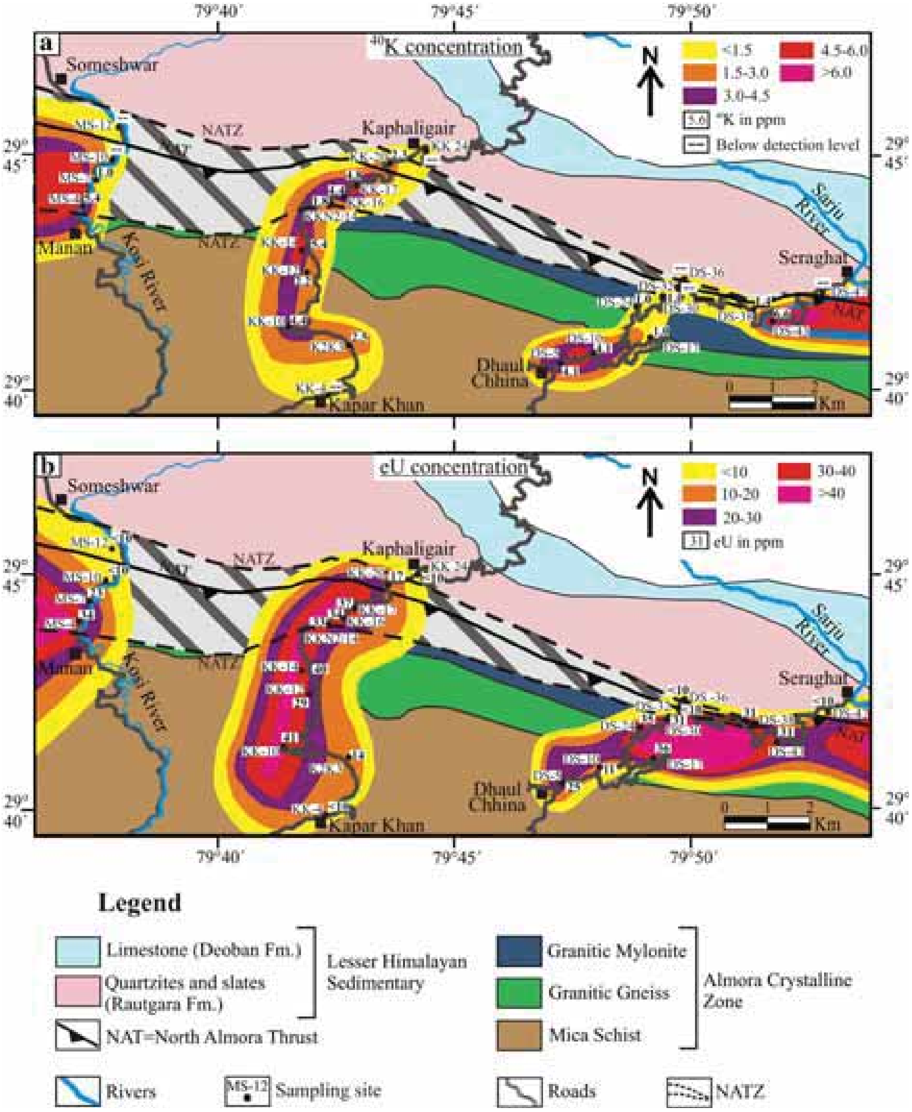

Figure 1. Geological map of the study area showing sample locations, major lithologies and the distribution of (**a**) ^{40}K and (**b**) eU near the North Almora Thrust Zone. (Modified after Joshi *et al.* 2017).

6.6 ppm, while the granitic gneiss and mica schist revealed intermediate ^{40}K concentrations between 2.2 and 5.4 ppm.

The distribution of eU is comparable to the distribution of ^{40}K. The Rautgara Formation reveals the lowest eU concentration in the area, <10 ppm. Higher eU is recorded in the Almora Group of rocks, with mica schist showing 11–25 ppm and quartzite and granitic gneiss presenting 40–41 ppm (figure 1b).

Similar to the low ^{40}K and eU, in the quartzites of the Rautgara Formation, the Ra(eU) concentration is very low, 2–5 ppm in some cases, and below the detection level in others (supplementary table 1). Among the ACZ rocks, the mica schist and the granitic gneiss reveal the lowest and the intermediate Ra(eU) concentration of 4–7 and 11 ppm, respectively, while the mylonite presents maximum Ra(eU) concentration, up to 19 ppm (figure 2a).

The highest Th concentrations, up to 46 ppm, are recorded in the mylonites of the Almora Group followed by the mica schist, 9–31 ppm (figure 2b). Th concentration is below the detection level in all except one sample of the quartzite of the Rautgara Formation.

In the study area, ^{40}K, U and Th show three spatially separated concentration zones (figures 1 and 2). These concentrations are defined by comparing the detected value of the radioisotopes with the known standards. The first zone is almost semicircular, occurring in the western part of the study

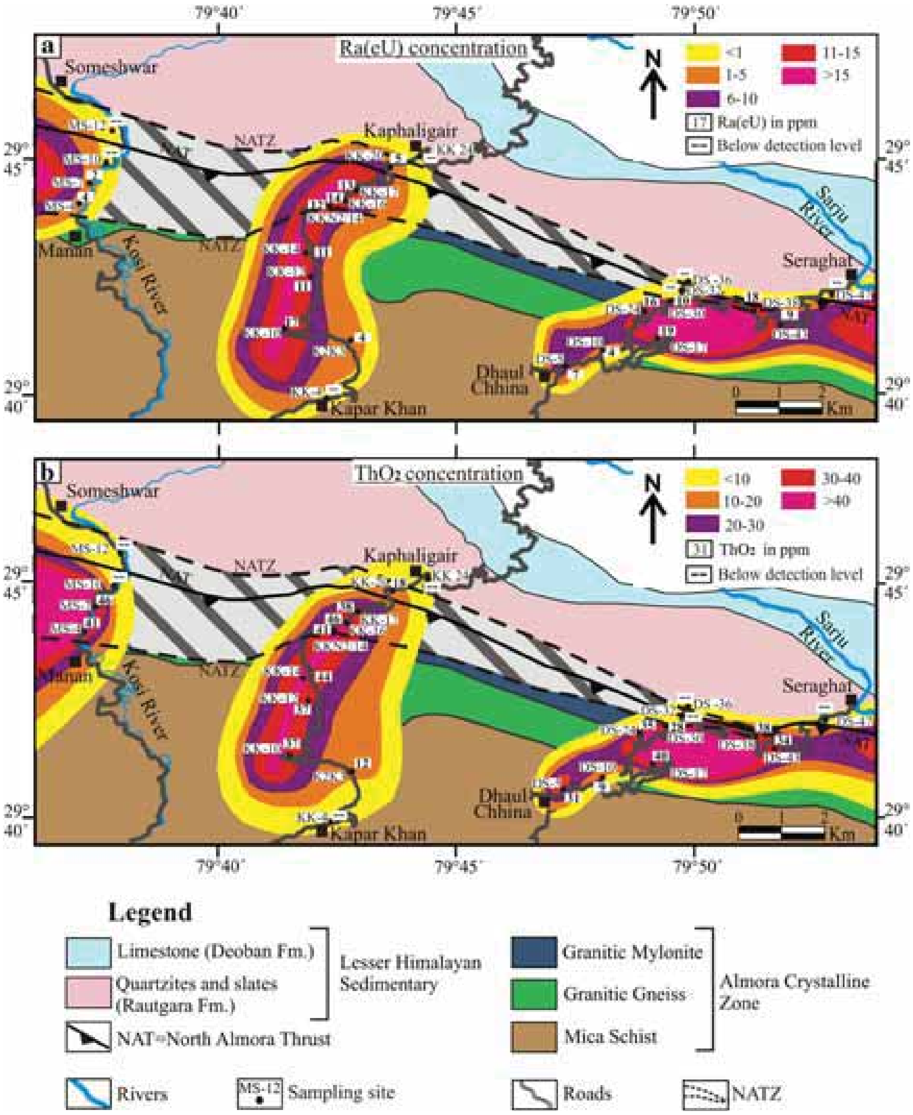

Figure 2. Geological map of the study area showing sample locations, major lithologies and the distribution of (**a**) Ra(eU) and (**b**) ThO_2 near the North Almora Thrust Zone. (Modified after Joshi *et al.* 2017).

area between Manan and Someshwar. The second zone is in the central part of the study area. It extends southwards from the Kaphaligair, starting at the northern boundary of the NATZ, to the north of the Kapar Khan. The third zone is in the eastern part of the area near Seraghat and Dhaul Chhina. Although the concentration zones are in the vicinity of the NATZ, their shape and spatial distribution with respect to each other reveal no direct control of the NATZ (figures 1 and 2).

4.2 *Relative enrichment of Ra(eU), ^{40}K and Th*

The relative enrichment of Ra(eU), ^{40}K and Th is examined by recalculating the abundance of Ra(eU), Th and ^{40}K to 100% and plotting them in a ternary diagram (figure 3). Mylonites are highly enriched with Th (63–81%) with some Ra(eU) (30–35%) and a minor amount of ^{40}K (12–15%). Granitic gneisses also show Th enrichment (>75%) with very little Ra(eU) (15–23%) and ^{40}K (10–12%) enrichment. Most quartzite samples have the radioisotope content below the detection level, except three samples, which is present in detectable amounts. The first one shows a trend towards the Th apex, with Th >90%, while both the others have 20% < Ra(eU) < 30% and ^{40}K $\sim$10%. Two samples of mica schist show a trend towards the Th apex (75% < Th < 88%) along with 10–15% of ^{40}K and 15–25% of Ra(eU), while one sample shows minor Ra(eU) and ^{40}K enrichment

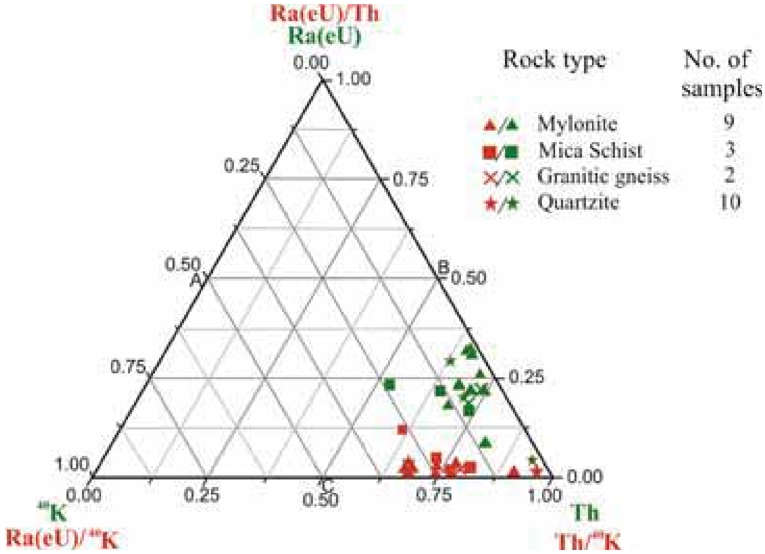

Figure 3. Ternary diagrams showing relative abundance of Ra(eU), ^{40}K and Th, and of their ratios (Ra(eU)/Th, Ra(eU)/^{40}K, Th/^{40}K).

(near 50% line BC). In general, all studied samples show the dominance of Th.

With respect to the ^{40}K and Ra(eU), Th concentration is much higher in the studied rocks (figure 3). Such behaviour is not uncommon. High relative concentration of Th is also reported from other parts of the Lesser Himalaya, such as the soil near Main Central Thrust (MCT) (Mukherjee *et al.* 2007). It is also known from other shear zones in India, namely, the Singhbhum shear zone (Banerjee *et al.* 2011). Other U-bearing granites and granitic rocks also show the relative high concentration of Th (e.g., Ashley 1984; Ali *et al.* 2012). The higher Th concentration in these cases is due to secondary mineralisation.

5. Discussion

Mylonite shows lower ^{40}K concentration, between 1 and 6.6 ppm, while the granitic gneiss and mica schist revealed intermediate ^{40}K concentrations between 2.2 and 5.4 ppm. The granitic mylonite and gneiss have higher U and Th concentration than the quartzite of the Rautgara Formation where the concentration is below the detection level (figures 1 and 2; supplementary table 1). Figure 3 reveals a relative enrichment of Th with some Ra(eU).

In summary, the studied rocks have ^{40}K concentration comparable to the continental crust; however, their Th and U concentrations are much higher (7.3 and 23.9 ppm, respectively) than the average upper crustal abundance (2.8 and 10.7 ppm).

5.1 *Enrichment of U at the NATZ*

The Kumaun Lesser Himalaya was formed by a general forelandward progression of thrusting along MCT, despite a few exceptions of out-of-sequence or reactivated thrusts (Srivastava and Mitra 1994; Yin 2006). Previous reports have indicated U and Th ore mineralisation in the shear zones within and near crystalline rocks of MCT and Ramgarh Porphyroids. These findings have led to the conclusion that over 60% of the MCT and Ramgarh Porphyroids terrain is favourable for the exploration of these radioisotopes (Mukherjee *et al.* 2007). The rocks here are mylonitised, and the mineralisation has been related to deformation-induced radioisotope remobilisation and the subsequent emplacement as veins (Mukherjee *et al.* 2007).

High soil gas radon (a daughter product of U) concentration is reported from granitic rocks in southern ACZ, i.e., Saryu Formation (Prasad *et al.* 2008). High radon values were also recorded in the vicinity of the NATZ, and are attributed to the increased mobilisation of U in the shear zone foliations as grain size reduction intensifies due to the increasing shear strain (Nashine *et al.* 1982).

The studied rocks of the ACZ were thrust from the Higher Himalayan granites along MCT (Valdiya 1980; Agarwal 1994; Yin 2006). The thrusting led to intense deformation and friction-related heat (e.g., Agarwal *et al.* 2011), which caused metamorphism up to amphibolite grade (Srivastava and Mitra 1996). This led to the formation of rocks such as the granitic mylonites, granitic gneisses and various kinds of schists (Bhattacharya and Agarwal 1985).

Hence, the rocks investigated here, may be enriched in U and Th similar to the rocks of MCT and Ramgarh Porphyroids due to the remobilisation of radioisotopes provoked by metamorphism (e.g., Mukherjee *et al.* 2007). Possibly, the radioisotopes diffused in the granitic protolith were remobilised and concentrated, during thrusting, in and around the NATZ. Features such as schistosity could play an important role in localising the radioisotopes concentration in the NATZ, similar to that in the southern part of the ACZ (e.g., Nashine *et al.* 1982; Choubey *et al.* 1999). In fact, thrusting and related deformation-causing enrichment of U is not a feature limited to the Himalayas, but is also reported from other shear zones outside the Himalaya. For example, enrichment is caused due to the introduction of U-bearing fluids or due to regional metamorphism by leaching of a uraniferous host rock, such as the granitic rocks of the Kinora–Vermilion Bay area in Canada, granite from the Laramie mountains, USA (Gundersen and Wanty 1971; Stuckless and Troëng 1984; Oliver *et al.* 1999; Banerjee *et al.* 2011).

5.2 *Spatial distribution of U with respect to the NATZ*

In the study area, the radioisotopes are distributed randomly. The distribution seemingly has no spatial relationship with the NATZ (figures 1 and 2). A similar heterogeneous distribution is reported in other Lesser Himalayan thrust systems, especially at MCT and is owed to multi-episodal deformation at the MCT (Mukherjee *et al.* 2007). Notably, a multi-episodal deformation comparable to the MCT and multiple thrust splays along the NATZ were recently recognised by Joshi *et al.* (2017). The radioisotopes may thus have been enriched throughout the various episodes of deformation at NATZ, along with different splays, leading up to a heterogeneous distribution.

6. Conclusions

The Th and U values in the studied rocks are higher (7.3 and 23.9 ppm, respectively) than the average values of the continental crust (supplementary tables 1 and 2). They are concentrated at the NATZ (figures 1 and 2). Among the three radioisotopes, Th has the highest concentration and Th/Ra(eU) varies between 2.1 and 23. The enrichment zones of U and Th do not show any spatial relation with the NATZ. Although the enrichment, at NATZ, is due to the mylonitisation and metamorphism up to amphibolite grade causing the remobilisation of radioisotopes, the heterogeneous distribution is a product of multi-episode deformation along multiple splays. In summary, the NATZ, in Kumaun Lesser Himalaya, provides a prospect of uranium mineralisation in the Lesser Himalaya.

Acknowledgements

GJ and KKA are thankful to the Head, CAS in Geology, Lucknow University, Lucknow, India for providing the working facilities. We thank the Director, Atomic Minerals Directorate for Exploration and Research, Department of Atomic Energy, for the gamma-ray spectrometric analysis. GJ is also thankful to CSIR, Government of India for providing financial support in the form of SRF, (09/107(0394)/2018-EMR-I). AA is thankful to Alexander von Humboldt Foundation and Deutscher Akademischer Austauschdienst for the financial support.

References

Acharyulu A A P S R, Murty B S and Bhaumik B K 2004 Enrichment characteristics of radioelements in various types of rock from Sambalpur district, Orissa, India; *J. Earth Syst. Sci.* **113** 321–352.

Agarwal K K 1994 Tectonic evolution of the Almora crystalline zone, Kumaun Lesser Himalaya: A reinterpretation; *J. Geol. Soc. India* **43**(**1**) 5–14.

Agarwal K K, Sharma A, Jahan N, Prakash C and Agarwal A 2011 Occurrence of pseudotachylites in the vicinity of South Almora Thrust Zone, Kumaun Lesser Himalaya; *Curr. Sci.* **101**(**3**) 431–434.

Agarwal A, Agarwal K K, Bali R, Prakash C and Joshi G 2016 Back-thrusting in Lesser Himalaya: Evidences from magnetic fabric studies in parts of Almora crystalline zone, Kumaun Lesser Himalaya; *J. Earth Syst. Sci.* **125** 873–884.

Agarwal K K, Bali R, Joshi G and Agarwal A 2017 A novel seahorse-shaped, small-scale structure from Almora Crystalline Zone, Uttarakhand, India; *Int. J. Earth. Sci. (Geol-Rundsch)*, https://doi.org/10.1007/s00531-017-1547-9.

Ali M, Shariff A A, Qamar N A and Laghar A 2012 Comparison of the Nagar Parkar (Pakistan) and Malani

(India) granites with reference to uranium and thorium abundances; *J. Him. Earth Sci.* **45**(**1**) 67–76.

Ashley P M 1984 Sodic granitoids and felsic gneisses associated with U–Th mineralization, Crockers Well, South Australia; *Minera. Deposita* **19** 7–18.

Banerjee K S, Guin R, Gutierrez-Villanueva J L, Charro M E and Sengupta D 2011 Variation in U-238 and Th-232 enrichment in U-mineralized zone and geological controls on their spatial distribution, Singhbhum Shear Zone of India; *Environ. Earth Sci.* **65** 2103–2110.

Bhattacharya A R and Agarwal K K 1985 Mylonites from the Kumaun Lesser Himalaya; *NeuesJahrb. Mineral.* **152** 65–77.

Bhola K L, Rama Rao Y N, Sastry C S and Mehta N R 1966 Uranium mineralization in Singhbhum thrust belt, Bihar, India; *Econ. Geol.* **61** 162–173.

Biswas A and Sharma S P 2016 Integrated geophysical studies to elicit the structure associated with uranium mineralization around South Purulia Shear Zone, India: A review; *Ore Geol. Rev.* **72** 1307–1326.

Choubey V M, Bartarya S K and Ramola R C 2000 Radon in Himalayan springs: A geohydrological control; *Env. Geol.* **39**(**6**) 523–530.

Choubey V M, Bist K S, Saini N K and Ramola R C 1999 Relation between soil gas radon variation and different lithotectonic units, Garhwal Himalaya, India; *J. Appl. Radiat. Isot.* **51** 587–592.

Cuney M 2009 The extreme diversity of uranium deposits; *Miner. Deposita* **44** 3–9.

Erdi-Krausz G, Matolin M, Minty B, Nicolet J-P, Reford W S and Schetselaar E 2003 *Guidelines for radioelement mapping using gamma-ray spectrometry data*; International Atomic Energy Agency Publication IAEA-TECDOC-1363, Vienna, Austria.

Florou H and Kritidis P 1992 Gamma radiation measurements and dose rate in the coastal areas of a volcanic island, Aegean Sea, Greece; *Radiat. Prot. Dosim.* **45**(**1**) 277–279.

Guagliardi I, Buttafuoco G, Apollaro C, Bloise A, De Rosa R and Cicchella D 2013 Using gamma-ray spectrometry and geostatistics for assessing geochemical behaviour of radioactive elements in the Lese catchment (southern Italy); *Int. J. Environ. Res.* **7**(**3**) 645–658.

Gundersen L C S and Wanty R B (eds) 1971 *Field studies of radon in rocks, soils, and water*; U.S. Geological Survey Bulletin, Washington, pp. 1–334.

Joshi G, Agarwal A, Agarwal K K, Srivastava S and Alva Valdivia L M 2017 Microstructures and strain variation: Evidence of multiple splays in the North Almora thrust zone, Kumaun Lesser Himalaya, Uttarakhand, India; *Tectonophys.* **694** 239–248.

Knoll G F 2000 *Radiation detection and measurement*; John Wiley & Sons, New York, 685p.

Kukreti B M and Sharma G K 2012 Performance analysis of gamma ray spectrometric parameters on digital signal and analog signal processing based MCA systems using NaI(Tl) detector; *Appl. Radiat. Isot.* **70** 901–905.

Mukherjee P K, Purohit K K, Saini N K, Khanna P P, Rathi M S and Grosz A E 2007 A stream sediment geochemical survey of the Ganga river headwaters in the Garhwal Himalaya; *Geochem. J.* **41** 83–95.

Nashine S K, Dhanaraju R, Bhatnagar G S and Narayan Das G R 1982 Uranium occurrences close to main central thrust around Sileth, Dhargaon, ChamyalaBalganga Valley, Tehri Garhwal (U.P.); *Him. Geol.* **12** 305–316.

Oliver N H S, Pearson P J, Holcombe R J and Ord A 1999 Mary Kathleen metamorphic-hydrothermal uranium – rare-earth element deposit: Ore genesis and numerical model of coupled deformation and fluid flow; *Austr. J. Earth Sci.* **46** 467–484.

Prasad Y, Prasad G, Gusain G S, Choubey V M and Ramola R C 2008 Radon exhalation rate from soil samples of South Kumaun Lesser Himalayas, India; *Radiat. Meas.* **43** 369–374.

Srivastava P and Mitra G 1994 Thrust geometries and deep structure of the outer and lesser Himalaya, Kumaun and Garhwal (India): Implications for evolution of the Himalayan fold and thrust belt; *Tectonics* **13** 89–109.

Srivastava P and Mitra G 1996 Deformation mechanisms and inverted thermal profile in the North Almora thrust mylonite zone, Kumaun Lesser Himalaya, India; *J. Struct. Geol.* **18** 27–39.

Stuckless J S and Troëng B 1984 Uranium mineralization in response to regional metamorphism at Lilljuthatten, Sweden; *Econ. Geol.* **79** 509–528.

Trivedi J R, Gopalan K and Valdiya K S 1984 Rb–Sr ages of granitic rocks within the Lesser Himalayan nappes, Kumaun, India; *J. Geol. Soc. India* **25** 641–654.

Valdiya K S 1980 *Geology of Kumaun Lesser Himalaya*; Wadia Institute of Himalayan Geology, Dehradun, India, 291p.

Yin A 2006 Cenozoic tectonic evolution of the Himalayan orogen as constrained by along-strike variation of structural geometry, exhumation history, and foreland sedimentation; *Earth-Sci. Rev.* **76** 1–131.

Corresponding editor: PULAK SENGUPTA